

Electronic Supplementary Information

Chain confinement promotes β -phase formation in polyfluorene-based luminescent ionogels

Rachel C. Evans^{a*} and Patricia C. Marr^b

^a School of Chemistry, Trinity College Dublin, Dublin 2, Ireland.

Tel: + 353 (0) 1 896 4215. Email: raevans@tcd.ie

^b School of Chemistry and Chemical Engineering, The Queens University of Belfast, The David Keir Building, Stranmills Road, Belfast, BT9 5AG, United Kingdom.

Tel: +44 (0) 28 90 975418. Email: p.marr@qub.ac.uk.

1. General

[Bmim]⁺ [NTf₂]⁻ was prepared at QUB using by published procedures.¹ TEOS (Sigma Aldrich) was used as purchased. All other reagents were used as commercially available. The conjugated polymers poly(9,9-di-*n*-octylfluorenyl-2,7-diyl)(PFO, Sigma-Aldrich, M_n = 15,834 g/mol, PDI = 3.7), poly[(9,9-dihexylfluorenyl-2,7-diyl)-*alt*-co-(2-methoxy-5-{2-ethylhexyloxy}-1,4-phenylene)] (PFPV, ADS Inc, M_n = 17,000 g/mol, PDI = 5.5.), poly[(9,9-di-*n*-octylfluorenyl-2,7-diyl)-*alt*-(benzo[2,1,3]thiadiazol-4,8-diyl)] (P8BT, Sigma-Aldrich, average M_n = 10,000-20,000 g/mol) and poly(9-vinylcarbazole) (PVK, Sigma-Aldrich, average M_n = 25,000-50,000 g/mol) were used without further purification.

Fourier Transform Infrared (FTIR) spectra were recorded on a Perkin-Elmer Spectrum 100 FTIR spectrometer at room temperature between 4000-400 cm⁻¹ with a resolution of 1 cm⁻¹. To obtain a reasonable signal to noise ratio the average of 64 scans was taken. Powder X-ray diffraction patterns were recorded using a Siemens D500 diffractometer using Cu K α radiation (λ = 1.54 Å) from 5-700° (2 θ). Solution phase photoluminescence spectra were measured on a Varian-Cary Eclipse fluorimeter. Solid-state photoluminescence spectra of the monolithic CP-ionogel samples were recorded on a Horiba-Jobin-Yvon Fluorolog-3 spectrometer using a Horiba-Jobin-Yvon integrating sphere. Emission and excitation spectra were corrected for the wavelength response of the system using correction factors supplied by the manufacturer. PL quantum yields were determined using the method previously described.² The experimental error is 10%. Appropriate excitation and emission wavelengths were selected for each system and the excitation and emission slit widths were both typically 1.0 nm. The effect of mechanical force on the optical properties of PFO-IG was investigated by grinding and pressing (~10 megagrams) a portion of the sample using a KBr die assembly.

Solid-state nuclear magnetic resonance (NMR) spectroscopy was conducted by the EPSRC service at the University of Durham. ¹³C and ²⁹Si were obtained using a Varian Unity Inova spectrometer operating at 75.40 MHz for ¹³C and 59.56 MHz for ²⁹Si.

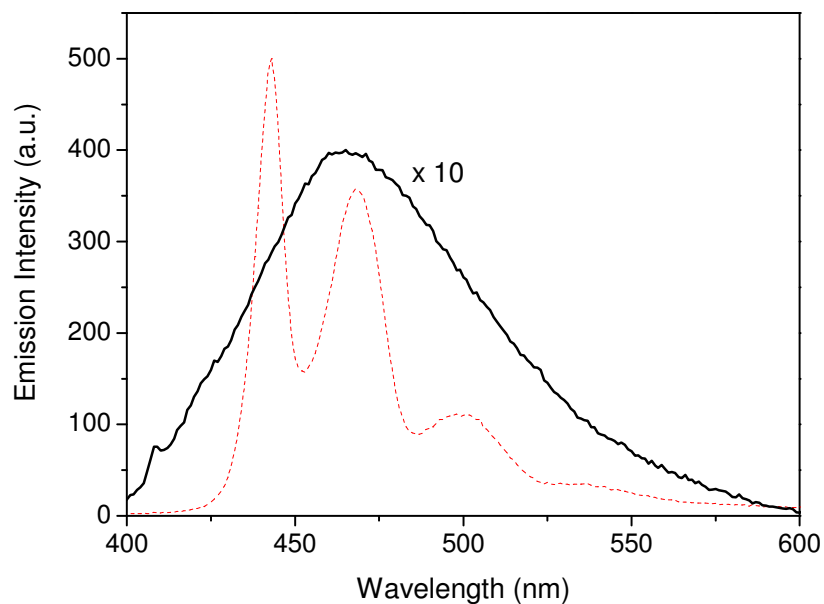


Figure S1. Room temperature photoluminescence spectrum of **BL-IG** (solid black line) excited at 370 nm (PLQY = 2.5%). To enable visual comparison with the **PFO-IG** spectrum (red dotted line), the emission data for **BL-IG** have been multiplied by a factor of 10.

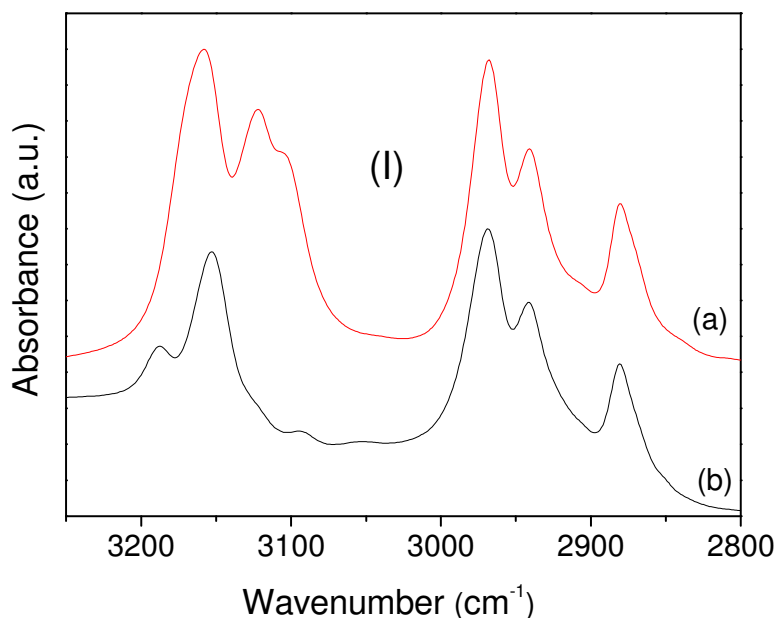


Figure S2. FTIR spectra of (a) neat RTIL and (b) **BL-IG** in the region 2850-3200 cm⁻¹. (I) corresponds to the region of the spectrum identified in Fig. 2.

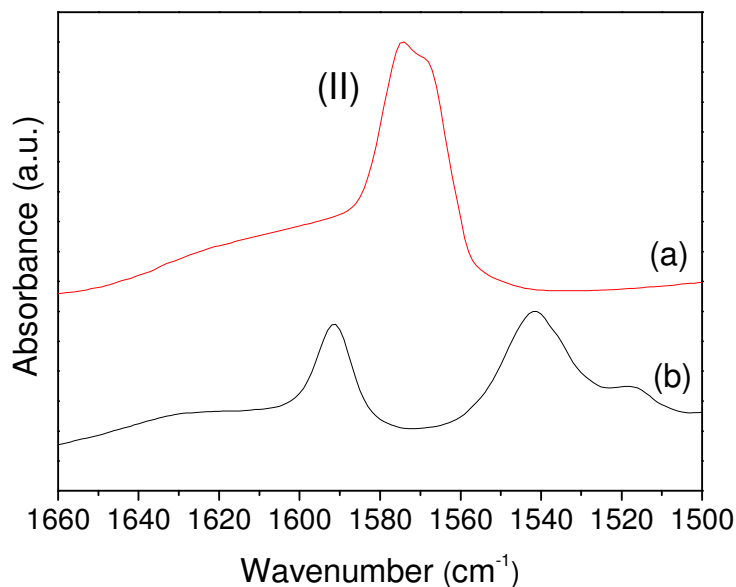


Figure S3. FTIR spectra of (a) neat RTIL and (b) **BL-IG** in the region 1500-1660 cm⁻¹. (II) corresponds to the region of the spectrum identified in Fig. 2.

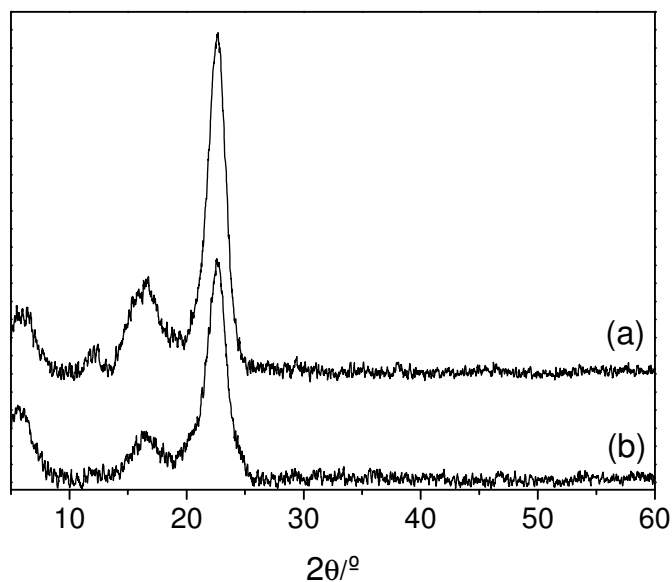


Figure S4. Powder XRD diffractograms of (a) **PFO-IG** and (b) **BL-IG**.

The powder XRD patterns are characteristic of an amorphous SiO₂ network. The peaks are assigned to (i) coherent diffracting regions within the siliceous network (~22.6°), (ii) an interparticle scattering interference (~4–6°) and (iii) in-plane ordering of intra-siloxane domains (~15–16°).³

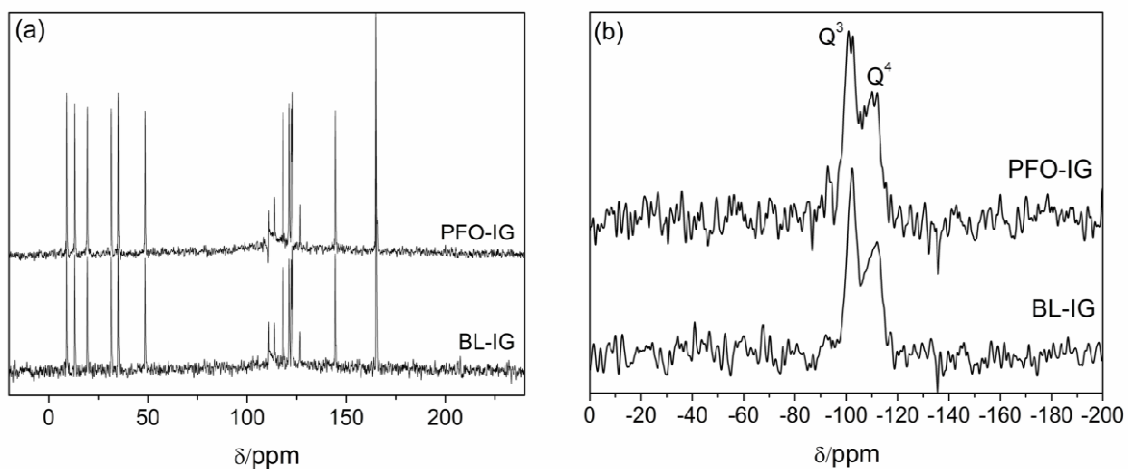
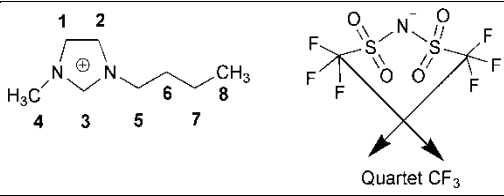


Figure S5. (a) ^{13}C MAS-NMR and (b) ^{29}Si MAS-NMR of **PFO-IG** and **BL-IG**.

NMR assignments:

	
^{13}C NMR of [Bmim][Ntf ₂] ₂ in CDCl ₃ . ⁴	^{13}C MAS NMR of BL-IG containing [Bmim][Ntf ₂] ₂
C1 123.7 ppm	C1 122.7
C2 122.0 ppm	C2 121.2
C3 137.7 ppm	C3 144.6
C4 36.4 ppm	C4 34.9
C5 49.6 ppm	C5 48.5
C6 32.1 ppm	C6 31.5
C7 19.3 ppm	C7 19.4
C8 13.1 ppm	C8 13.0
	CF ₃ Quartet (113.8, 118.1, 122.3, 126.6 ppm)
	Methanoic acid (formic acid) 164-165 ppm

The ^{29}Si MAS-NMR spectra (Fig S5b) of PFO-IG and BL-IG both exhibit broad signals characteristic of Q³ ($\equiv\text{SiO}$)₃SiOH (~102 ppm) and Q⁴ ($\equiv\text{SiO}$)₄Si (~111 ppm) units, indicating the presence of a silica network composed mainly of cyclic units cross-linked by oxygen bridges.⁵

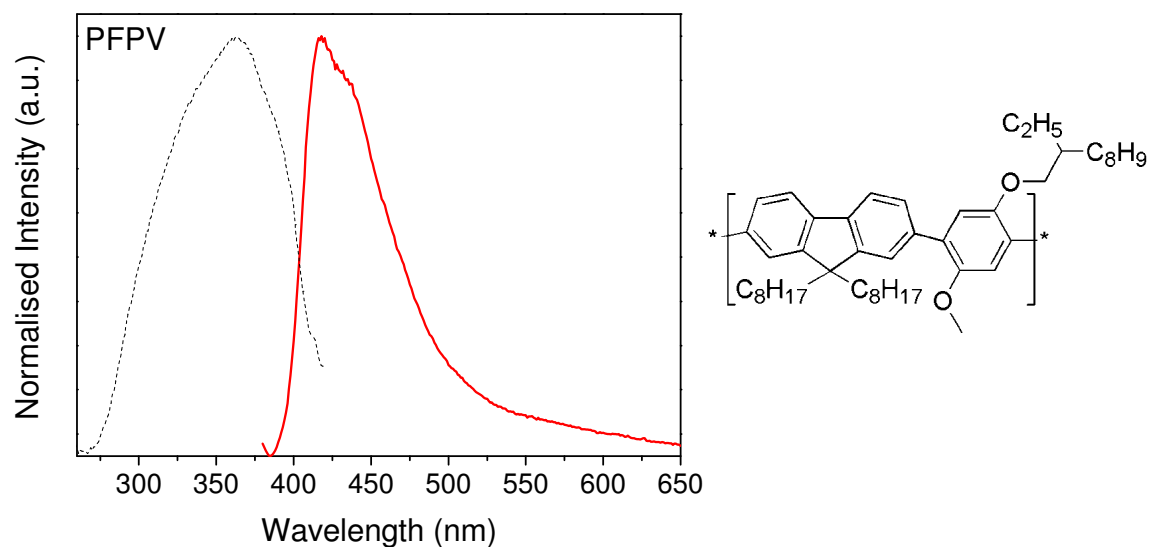


Figure S6. Room-temperature photoluminescence ($\lambda_{\text{ex}} = 370$ nm, solid red line) and excitation spectra ($\lambda_{\text{em}} = 440$ nm, dashed black line) for **PFPV-IG**. PLQY = 4.2%.

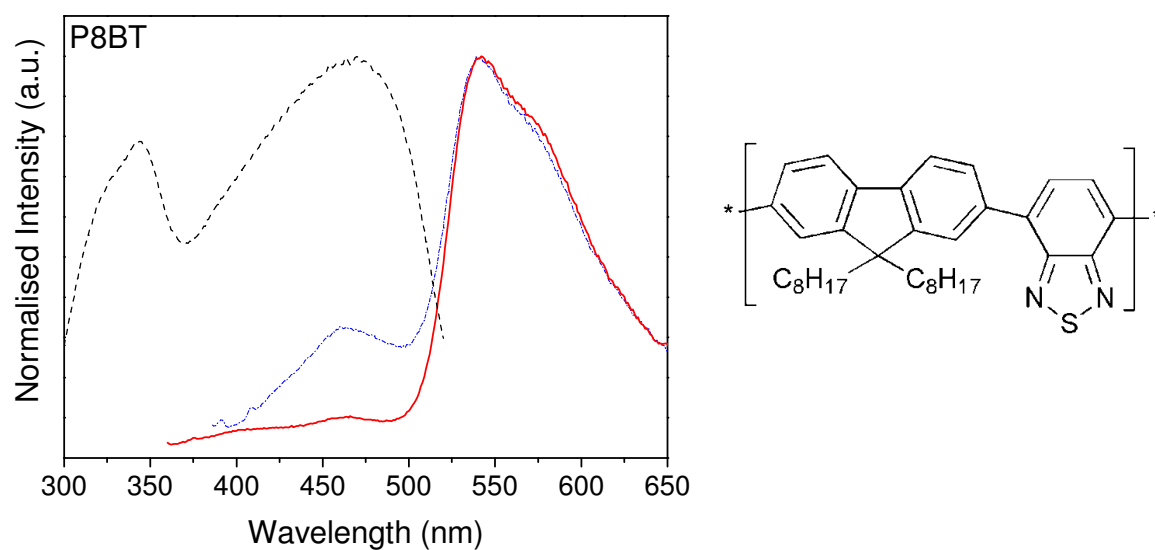


Figure S7. Room-temperature photoluminescence and excitation spectra for **P8BT-IG**. PL spectra are shown for selective excitation of the benzothiadiazole ($\lambda_{\text{ex}} = 350$ nm, solid red line) and fluorene ($\lambda_{\text{ex}} = 370$ nm, blue dotted line) units. The excitation spectrum was recorded in the benzothiadiazole emission band at 540 nm (black dashed line) and reveals two maxima at *ca.* 348 and 368 nm, indicating energy transfer from the fluorene to the benzothiadiazole unit must contribute to this emission. PLQY = 7.5%.

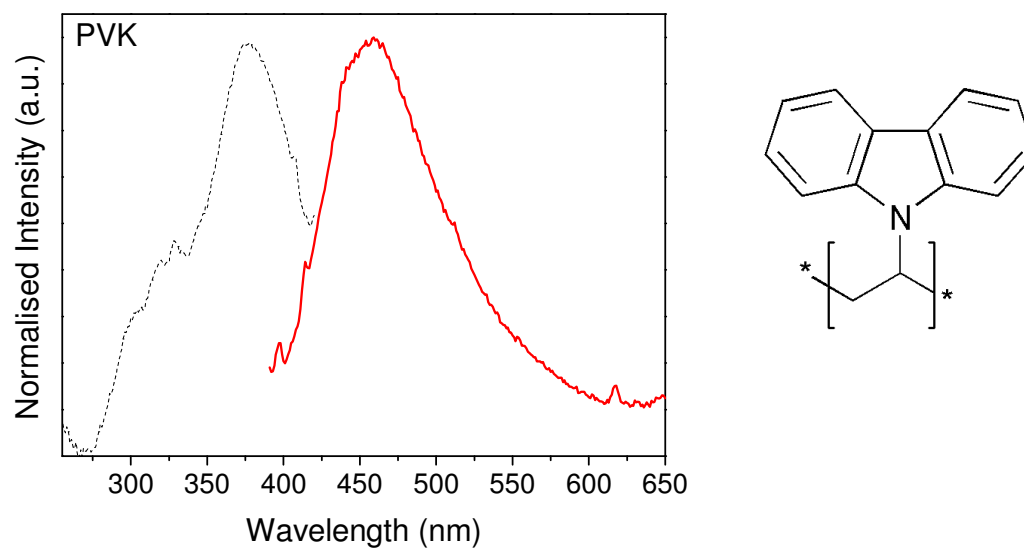


Figure S8. Room-temperature photoluminescence ($\lambda_{\text{ex}} = 370$ nm, solid red line) and excitation ($\lambda_{\text{ex}} = 460$ nm, dashed black line) spectra for **PVK-IG**. PLQY = 2.2%

IL ν (cm ⁻¹)	BL-IG ν (cm ⁻¹)	PFO-IG ν (cm ⁻¹)	Assignment
	574	571	Si–O–Si bend
616	617	618	Ring CNC op bend
655	660	698	Ring ip str.
739	739	741	Ring ip bend, CH ₂ (N) and CH ₃ (N)CN bend, CF ₃ sym. bend, ring ip HCCH.
760	757	761	Ring HCCH asym. bend, SNS sym. str.
791	790	791	Ring HCCH asym. bend, CS str.
846	955	647	
1059	1060	1059	Ring ip asym. str., CC str. NCH ₃ twist
1139	1143	1138	CC str.
1192	1195	1194	Ring sym str., CH ₂ (N) and CH ₃ (N)CN str., CF ₃ asym. str.
1227	1357	1351	Ring ip sym. str., CH ₂ (N) and CH ₃ (N)CN str.
1421	1421	1425	Ring ip sym. str., CH ₃ (N) str., CH ₃ (N)HCH sym. bend or NC(CH ₃)NHCH sym. bend.
1469	1466	1470	Ring ip sym. str., CH ₃ (N)CN str.
	1538	1541	NC(CH ₃)NCN str.
1575	1596	1590	Ring ip sym./asym. str., CH ₂ (N) and CH ₃ (N)CN str.
2879	2880	2879	Terminal CH ₃ HCH sym. str.
2940	2939	2941	CH ₂ sym. str., CH ₃ asym. str.
2968	2966	2968	CH ₂ HCH asym. str.
3104	-	-	
3121	-	-	Ring CH str.
3159	3153	3151	Ip and op C4,5-H str.
-	3187	3184	C4,5-H str.
-	3400	3400	Si-OH str.
	(broad)	(broad)	

Table S1. Observed IR bands of RTIL, **PFO-IG** and **BL-IG**. Frequency (ν) and vibrational assignments: sh (shoulder), ip (in-plane), op (out-of-plane), sym (symmetric), asym (asymmetric). Assignments from Ref. ^{6,7} and references therein.

References

1. P. Bonhôte, Ana-Paula Dias, N. Papageorgiou, K. Kalyanasundaram, and M. Grätzel *Inorg. Chem.*, 1996, **3**, 1168.
2. J. Pina, H. D. Burrows, R. S. Becker, F. B. Dias, A. L. Maçanita and J. S. de Melo, *J. Phys. Chem. B.*, 2006, **110**, 6499.
3. L. S. Fu, R. A. S. Ferreira, N. J. O. Silva, L. D. Carlos, V. d. Z. Bermudez and J. Rocha, *Chem. Mater.*, 2004, **16**, 1507.
4. S. Hesse-Ertelt, T. Heinze, B. Kosan, K. Schwikal, F. Meister *Macromol. Symp.* 2010, 294-II, 75.
5. G. Engelhardt, in *Encyclopedia of Magnetic Resonance.*, 2007.
6. K. Noack, P. S. Schulz, N. Paape, J. Kiefer, P. Wasserscheid and A. Leipertz, *Phys. Chem. Chem. Phys.*, 2010, **12**, 14153.
7. M. P. Singh, R. K. Singh and S. Chandra, *Chem. Phys. Chem.*, 2010, **11**, 2036.